Growth Enhancement of Organic Nonlinear Optical Crystals by Femtosecond Laser Ablation

*Hozumi Takahashi[1,2], Mayu Yamaji[1,2], Jun Ikeyama[1], Makoto Nakajima[3], Hideaki Kitahara[3], Syouei Tetsukawa[3], Naritaka Kobayashi[4], Mihoko Maruyama[5-7], Teruki Sugiyama[2,8,9], Shuji Okada[10], Yusuke Mori[5], Seiichiro Nakabayashi[1,4], Masashi Yoshimura[3] and Hiroshi Y. Yoshikawa[1,3-5]**

[1]Department of Chemistry, Saitama University, Shimo-okubo 255, Sakura-ku, Saitama 338-8570, Japan

[2]Department of Applied Chemistry and Center for Emergent Functional Matter Science, National Yang Ming Chiao Tung University, Hsinchu 30010, Taiwan

[3]Institute of Laser Engineering (ILE), Osaka University, 2-6 Yamada-oka, Suita, Osaka 565-0871, Japan

[4]Division of Strategic Research and Development, Graduate School of Science and Engineering, Saitama University, Shimo-okubo 255, Sakura-ku, Saitama 338-8570, Japan

[5]Graduate School of Engineering, Osaka University, 2-1 Yamada-oka, Suita, Osaka 565-0871, Japan

[6]Institute for Advanced Co-Creation Studies, Osaka University, 2-1, Yamadaoka, Suita City, Osaka 565-0871, Japan

[7]Graduate School of Life and Environmental Science, Kyoto Prefectural University, Kyoto, Kyoto 565-0871, Japan

[8]Center for Emergent Functional Matter Science, National Chiao Tung University, Hsinchu, 30010, Taiwan

[9]Division of Materials Science, Graduate School of Science and Technology, Nara Institute of Science and Technology, Ikoma 630-0192, Japan

[10]Graduate School of Organic Materials Science, Yamagata University, 4-3-16 Jonan, Yonezawa 992-8510, Japan

AUTHOR INFORMATION

Corresponding Author

*Email: hiroshi@mail.saitama-u.ac.jp

ABSTRACT

The impact of femtosecond (fs) laser ablation on the shape and nonlinear optical (NLO) properties of organic crystals was investigated. Fs laser ablation of a local region of a NLO crystal can selectively enhance the growth of targeted faces. Reflection imaging of crystal surfaces revealed that a number of new crystal steps are generated from ablated area, which induces the crystal growth enhancement. In addition, the evaluation of terahertz (THz) wave emission from ablated crystals shows that NLO properties are not deteriorated after fs laser ablation. We foresee that crystal shape control by such a damage-less ablation process will potentially improve the NLO properties of organic crystals.

KEYWORDS Laser ablation, Organic nonlinear optical crystal, Crystal growth control, Terahertz wave emission, Spiral growth, Optical microscopy

MAIN TEXT

INTRODUCTION

Organic NLO crystals exhibit much more superior nonlinearity compared to inorganic materials and can potentially be applied to next-generation communication and medical devices such as THz-wave generation devices, second harmonic generator[1-2] and high-speed electric field sensors.[3-4] In particular, 4-dimethylamino-*N*-methyl-4-stilbazolium tosylate (DAST) and 4-dimethylamino-*N*-methyl-4-stilbazolium *p*-chlorobenzenesulfonate (DASC) are promising because of their significantly large NLO susceptibilities.[5] However, the preparation of DAST and DASC crystals that are suited to industrial applications is not trivial because their NLO properties strongly depend on crystal shape.[5-7] Matsukawa et al. reported that THz waves output intensity of DAST and DASC crystals increased up to a thickness to some extent when velocity-matching conditions were satisfied.[5] Brahadeeswaran et al. reported that ultrathin DASC crystals could generate THz wave with relatively higher efficiencies, especially at higher frequencies.[6] Thin and large DASC crystals are stable for two-dimensional THz imaging, as studied by Serita and co-workers.[7] These works clearly suggest that organic NLO crystals with desired shapes is required for their applications. So far, researchers have tried to obtain such crystals by adjusting conventional crystallization parameters such as concentration, solvent, and temperature.[5-6, 8-9] However, further improvement of NLO properties of organic crystals is challenging even with the systematic screening of the parameters.

Recently, our group has developed an innovative method that can promote growth of targeted crystal faces by modifying crystal structure via fs laser ablation.[10-12] In this method, fs laser ablation of the local area ($< 1\ \mu m^2$) on a crystal surface can induce the formation of screw dislocation, which lead to the generation of energetically advantageous growth mode, called as

spiral growth. By using this method, we succeeded in producing crystals of proteins and amino acids with specific shapes that cannot be made by adjusting the conventional parameters alone. Since spiral growth is one of the fundamental growth modes that can appear for various materials,[13] we expect the laser ablation methods may allow for the production of organic NLO crystals with desired shapes.

In this work, we have investigated the impact of the fs laser ablation method on shape and NLO properties of DAST and DASC crystals. We systematically monitored the change in crystal shapes after fs laser ablation. The molecular-level crystal growth dynamics before and after fs laser ablation was observed by bright field microscopy and advanced reflection microscopy. Finally, the influence of laser ablation on crystal quality and NLO properties was assessed by polarized microscopy and by measuring THz wave generation.

EXPERIMENTAL METHODS

DAST powder from Dai-Ichi Pure Chemicals Co. (Japan) or Kanto Chemical Co. (Japan) was used. DASC was synthesized by the previously reported method.[14] Powder of DAST (10.8 mg) or DASC (4.5 mg) was added to a glass vial (NICHIDEN-RIKA GLASS CO., LTD.) with 3 mL of ethanol solvent (Wako, >99.5%). Then, the powder was completely dissolved by vigorously shaking the mixture at 55 ºC for at least 10 hours in an incubator (IN604, Yamato) with a shaker (MMS-210, EYELA). Afterwards, the sample was cooled down from 55 ºC to 23 ºC with a rate of 5 ºC per hour. For crystallization, the solution was put onto a cover glass with a silicon rubber spacer (thickness: 1.5 ± 0.2 mm). Then the chamber was immediately sealed with another cover glass to avoid evaporation of the solution. The chamber was placed on a temperature-controlled stage (20ºC) that was installed on an inverted type of a laser-scanning confocal microscope (A1R

MP+, Nikon). After spontaneous nucleation occurred (typically within 10 min), a single femtosecond laser pulse from a regeneratively amplified Ti:Sapphire laser system (λ = 800 nm, $\Delta\tau$ ~ 100 fs, Legend Elite, Coherent) was shot to a crystal surface through an objective lens (20×, N.A. 0.5, Plan Fluor, Nikon). The laser energy was adjusted by a half-wave plate and a polarizer. The focal diameter calculated by the Rayleigh's criterion (~ 1.22λ/N.A.) is around 2 μm. In this work, to indeed induce laser ablation of crystals without significant damage, the laser energy was set between 1.2 to 7.6 times larger than the threshold laser energy, E_{th}, for laser ablation of DAST (E_{th} = 13 nJ/pulse) and DASC (E_{th} = 67 nJ/pulse) crystals. E_{th} was determined by using the previously reported model where ablation area increases logarithmically with laser energy because of the Gaussian-like spatial distribution of the laser beam[15] (Figure S1). The crystal growth dynamics was observed by bright field and reflection microscopies. In particular, the reflection microscopy was based on a laser confocal microscope combined with a reflection microscope (LCM-RM) or combined with a differential interference contrast microscope (LCM-DIM), which allows for the visualization of crystal steps with the height of ~ nm.[16-17] To avoid optical absorption by DAST and DASC, a red laser (λ = 638 nm) was used for the observation with the bright-field and interferometric microscopies. The optical setup was shown in Figure S2. ImageJ software (NIH) was used for image analysis and adjusting image contrast. Crossed Nicols images were gained by an upright type of a polarization microscope (ECLIPSE LV100N POL, Nikon). The THz wave spectra were obtained by the Fourier transform of the measured waveforms using a femtosecond pulse laser (λ = 800 nm, $\Delta\tau$ ~ 100 fs, repetition rate of 80 MHz, Tsunami, Spectra Physics) at room temperature.[18-20] The excitation conditions were the power of 30 mW and the excitation beam spot of ~ 100 μm. The dipole-type low-temperature grown GaAs photoconductive antenna was used as a detector.

RESULTS AND DISCUSSION

Figure 1 shows representative examples of the growth behavior of DAST and DASC crystals when a single fs laser pulse was shot to the place close to the edge of the (001) surface, named as Face-I, at $t = 0$ (see also Movie S1 and S2). Before the laser shot, DAST and DASC crystals showed anisotropic crystal growth where the two faces always grow faster than the other two face, which has been also reported for various polar organic molecules.[21] Upon the laser ablation, the crystals showed the enhanced growth in the direction perpendicular to Face-I (defined as Face-I axis), whereas the non-irradiated face (defined as Face-II) did not (Figure 1(a) and 1(b) left, their magnified images are also shown in Figure S3(a) and S3(b)). Reflection images clearly show that a number of steps were generated and propagated from the ablated area (see also Movie S1 and S2). The corresponding time course plots clearly show sudden jumps of the growth along Face-I axis upon laser ablation, whereas the growth both along Face-I and Face II axis was almost constant before laser ablation and as-grown crystals (Figure 1(a), 1(b) right, and Figure S4 right). The average growth rate along Face-I axis for the first 20 mins after laser ablation was approximately 0.67 μm/min (DAST) and 1.15 μm/min (DASC), which are 3.63 times and 1.77 times larger than that for 20 mins before laser ablation, and they were 9.66 times and 1.83 times larger than that in the direction perpendicular to Face-II (defined as Face-II axis), respectively.

Figure 2 shows the growth behavior of DAST and DASC crystals when a single fs pulse was shot to the inward of (001) surface (see also Movie S3 and S4). The reflection images showed no particular step advancing before laser ablation. Then new crystalline steps were generated from the ablated area after laser ablation and propagated to the surrounding (Figure 2(a) and 2(b) left, Figure S5(a) and S5(b)). The corresponding time course plots clearly showed a significant jump of the crystal thickness upon laser ablation, whereas it was almost unchanged without laser ablation

(Figure 2(a) and 2(b) right, and Figure S4 right). The thickness was increased approximately from 2.0 to 3.7 μm (DAST) and from 3.5 to 4.8 μm (DASC) by laser ablation, which are 85% and 37% larger than those before laser ablation, respectively. Besides, although growth enhancement after laser ablation was very small compared to the case of the laser shot to a crystal edge (Figure 1), the crystal showed slight enhanced growth in both Face I and Face II directions (Figure S6) (Here both Face I and Face II are non-irradiated crystal faces). The average growth rate along Face-I axis and Face-II axis for the first 20 mins after laser ablation was approximately 0.05 μm/min (DAST) and 0.51 μm/min (DASC), which are 1.62 times and 1.17 times larger than that for 20 mins before laser ablation, respectively.

The results of Figure 1 and Figure 2 indicate that laser ablation can enhance growth of organic NLO crystals, and the enhanced direction depends on the location of a focal spot. When a focal spot was close to the edge of (001) surface, crystal growth was enhanced anisotropically toward the irradiated edge, which resulted in the change of a crystal shape from square to rectangle. On the other hand, when a fs laser pulse was shot to the inward to (001) surface, the crystal showed the growth enhancement especially toward perpendicular to the (001) surface, that is, ablated crystals became thicker. The inward shot also slightly enhanced growth along Face-I and Face-II axis and then became larger with its original square shape. We found that the focal spot position within approximately 5~10 μm from the edge of (001) surface can induce the anisotropic crystal growth. This may be because the shape of DAST and DASC crystals resemble a trapezoid from a side view (the angle of side face toward glass surface is ~70º for DAST and ~85º for DASC crystals, respectively), so that crystal thickening may slightly influence the increase in the crystal length along Face-I and Face-II axis. Alternatively, the side face (Face I) of a crystal might be ablated even if fs laser is shot at to some extent inward of (001) plane.

Figure 3 shows statistical data about the probability of crystal growth enhancement and step generation by fs laser ablation. Here, to clearly identify the effect of laser ablation, we determined the probability of growth enhancement in the following manner. In the case of the laser shot to a place close to the edge of (001) surface, we defined that crystal growth was enhanced when the crystal growth rate along Face-I axis became more than 1.5 times larger than that of Face-II axis for the first 20 - 30 mins after laser ablation. On the other hand, in the case of laser shot to the inward of (001) surface, we defined that crystal growth was enhanced when the growth rate for the first 20 - 30 mins along Face-I axis and Face-II axis was increased by more than 10 % compared to that for 20 - 30 mins before laser ablation. The statistical analysis yields the probability of the growth enhancement by fs laser ablation for the edge shot case to be approximately 43% (3/7) for DAST crystals and 60% (3/5) for DASC crystals (growth rate along Face-I axis after laser ablation: 0.29 ± 0.26 μm/min for DAST and 0.60 ± 0.39 μm/min for DASC crystals). On the other hand, those for the inward shot case were approximately 26% (6/23) for DAST crystals and 11% (1/9) for DASC crystals (averaged growth rate along Face-I and Face-II axis after laser ablation: 0.053 ± 0.050 μm/min for DAST crystals and 0.51 μm/min for DASC crystals). These probabilities are coincidentally comparable to that of the case of protein crystals (~ 30 %).[10] Furthermore, from the reflection images, we found that all the crystals of which growth was enhanced via fs laser ablation showed step generation from the ablated area, while the probability of step generation by laser ablation for all crystals (including those of which growth was not enhanced by the definition of this study) is approximately 63% (19/30) for DAST crystals and 100% (14/14) for DASC crystals, respectively. In fact, increase in crystal thickness with more than 1 μm for the first 120 minutes after laser ablation were observed with the probability of 23% (5/22) for DAST and 60% (3/5) for DASC crystals, respectively (Figure S7). These results clearly

indicate that fs laser ablation can induce the step generation from the ablated area, which plays an important role in enhancing the growth of organic NLO crystals.

The underlying mechanism of the growth enhancement of DAST and DASC crystals triggered by the step generation via fs laser ablation is probably attributed to changes in crystal growth mode, which are also reported for the case of crystals of protein and amino acids.[10-12] In general, at relatively low supersaturation, crystals without defects grow according to two-dimensional (2D) nucleation mode where crystals grow three-dimensionally by adding new 2D, molecularly thin islands on top of pre-existing 2D islands.[22] However, crystal growth becomes drastically slow (or stops) when supersaturation becomes insufficient for nucleation of 2D islands. On the other hand, we reported that fs laser ablation of crystals of proteins and amino acids could switch the growth mode from 2D nucleation growth to spiral growth, which is more energetically advantageous because of providing non-vanishing steps from screw dislocations.[10-12] Actually, in this work, we also found that the generation of spiral-like circular steps from the ablated area of DAST crystals sometimes appeared after fs laser ablation (Figure 4, see also Movie S5). Although clear spiral-like steps and 2D islands were not always detected, we found that a number of steps were generated and propagated from the ablated area to the surrounding in many cases (see probability of step generation in Figure 3). This fact strongly indicates that fs laser ablation induces energetically favorable growth mode such as spiral growth mode and/or other growth modes (e.g., peculiar 2D hillock with consecutive layers),[23] which results in the growth enhancement towards the irradiated face (Figure 1 and 2). These results suggest that fs laser ablation provide us a new approach to the control of shape of NLO crystals without changing environmental parameters such as temperature and concentration.

Finally, we assessed the NLO property of DAST and DASC crystals where laser ablation was induced during growth. Here, we evaluated the THz wave generation, which is one of the promising NLO properties of DAST and DASC crystals[5, 24-25] to examine whether laser ablation of deteriorate their NLO properties. Figure 5(a) and 5(b) shows THz Fourier-transformed spectra generated from as-grown and laser-irradiated DAST and DASC crystals. The thickness of crystals was approximately 6.8 μm (as-grown DAST crystal), 11.2 μm (laser-irradiated DAST crystal), 5.5 μm (as-grown DASC crystal), and 3.0 μm (laser-irradiated DASC crystal), respectively. Both as-grown and the laser-irradiated crystals showed a peak of THz wave generation around 1 THz with a dip around 1.1 THz, which is attributed to the characteristic absorption band of DAST and DASC crystals. This result indicates that the function of THz generation by DAST and DASC crystals are retained even after fs laser ablation. As studied in our previous studies by X-ray diffraction measurement[10] and polarization microscopy[11-12], laser-induced screw dislocations are localized at the ablated area and thus do not deteriorate crystal quality in a macroscopic scale. In fact, the etched diameter of DAST and DASC crystals was a few micrometers. On the other hand, the excitation beam spot for THz wave emission was approximately 100 μm. Besides, we could not also detect the significant deterioration of the single crystallinity of DAST and DASC under Crossed Nicols conditions (Figure S8 left). The whole area of ablated DAST and DASC crystals showed the same extinction angle as those before laser ablation (Figure S8 right). Such a damage-less ablation process should contribute to the crystal growth enhancement without the loss of NLO property.

CONCLUSION

We have revealed that fs laser ablation can enhance the growth of DAST and DASC crystals without losing their NLO properties. Fs laser ablation can induce the generation of a number of crystalline steps, which results in the enhancement of crystal growth. We confirmed that fs laser ablation of crystals does not leads to the deterioration of THz wave generation properties. In the future, we expect that the laser ablation method enables us to produce organic NLO crystals with desired shapes, which will drastically improve the NLO properties that cannot be achieved by conventional methods alone.

FIGURES

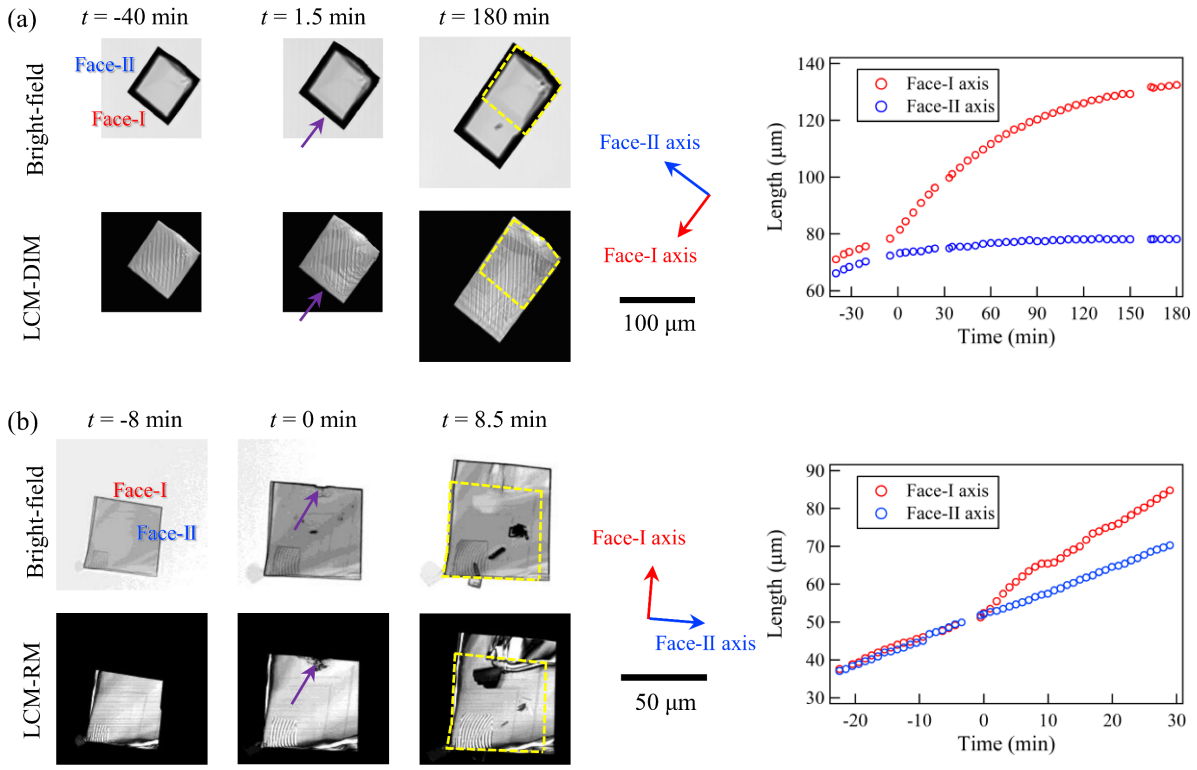

Figure 1. Enhancement of crystal growth by the laser shot to the edge of (001) surface. Representative growth dynamics of (a) a DAST crystal and (b) a DASC crystal before and after fs laser irradiation is shown. A single fs laser pulse was shot at $t = 0$. The laser energy was set to 100 nJ/pulse (~ 7.6 × E_{th}) for DAST and 300 nJ/pulse (~ 4.5 × E_{th}) for DASC. Red and blue arrows indicate the Face-I axis and Face-II axis, respectively. The purple arrow shows a focal point. The yellow dashed line in the microscopy images was the crystal shape at $t \sim 0$. The plots of crystal length as a function of time are shown in the right part.

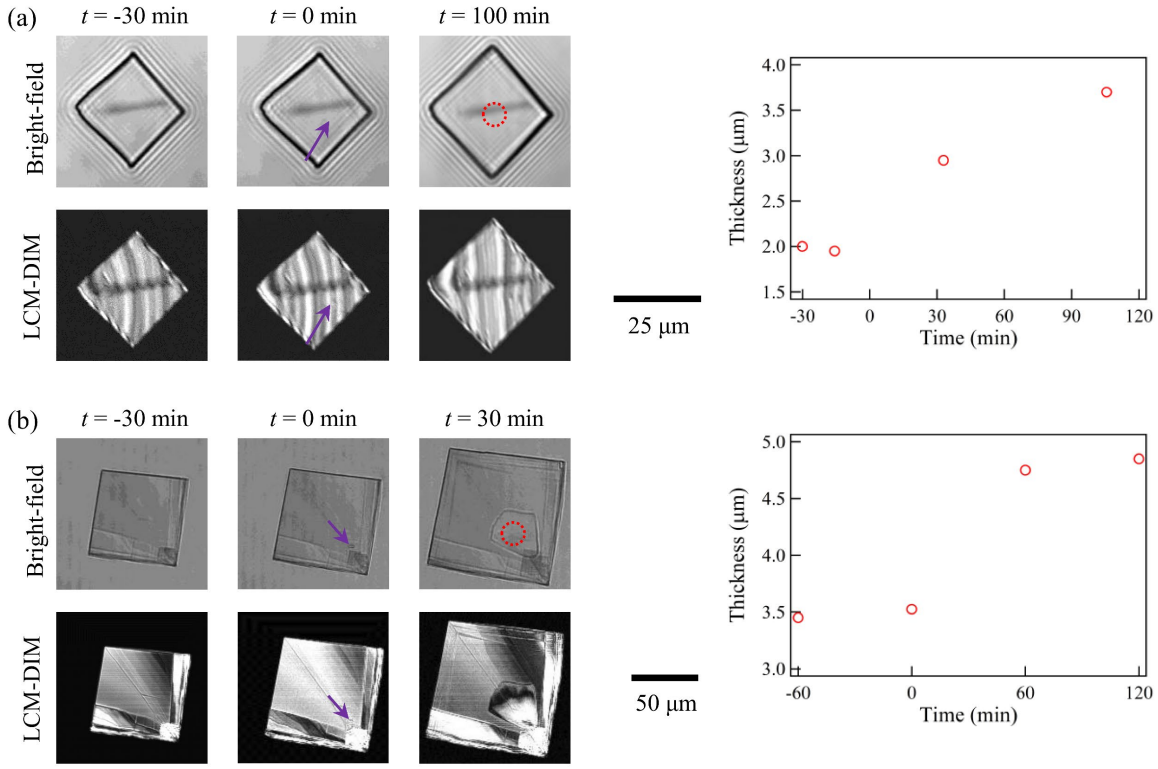

Figure 2. Enhancement of crystal growth by fs pulse laser shot to the inward of (001) surface. Representative growth dynamics of (a) a DAST crystal and (b) a DASC crystal before and after fs laser irradiation is shown. A single fs laser pulse was shot at $t = 0$. The laser energy was set to 30 nJ/pulse (~ 2.3 × E_{th}) for DAST and 80 nJ/pulse (~ 1.2 × E_{th}) for DASC. The purple arrow shows a focal point. The plots of crystal thickness as a function of time are shown in the right part. The crystal thickness of the region marked with red circles was measured.

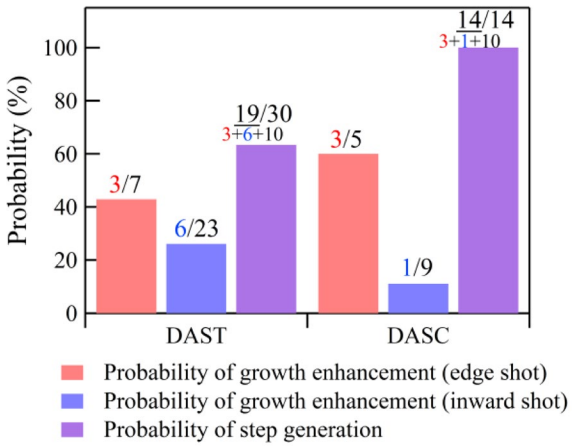

Figure 3. Statistical data about the probability of the crystal growth enhancement (red and bule) and step generation (purple) induced by fs laser ablation.

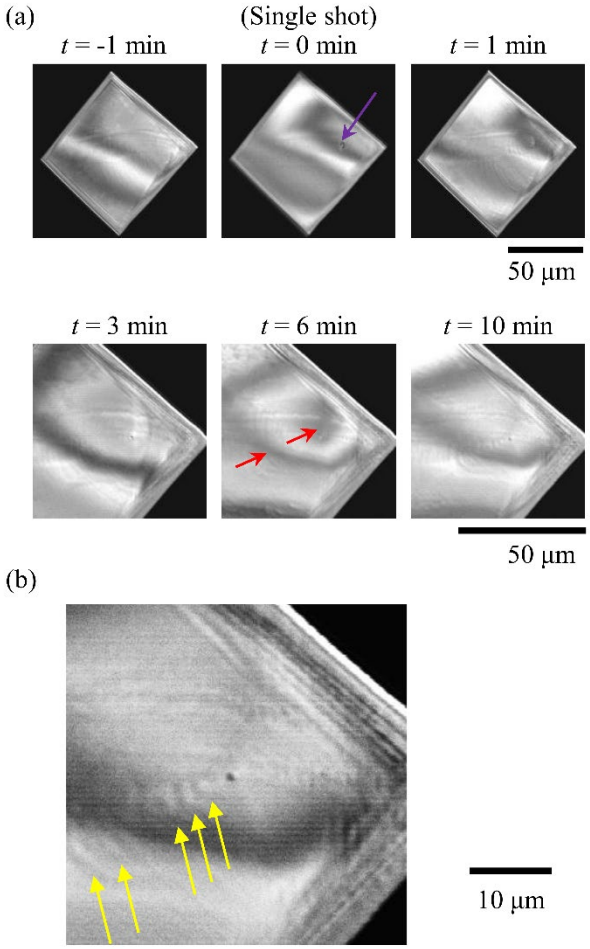

Figure 4. LCM-DIM images of the (001) surface of the laser-irradiated DAST crystal. A single fs laser pulse (30 nJ/pulse, ~ 2.3 × E_{th}) was shot at t = 0. The purple arrow shows a focal point. The yellow arrows indicate steps generated by fs laser ablation. The fringes with larger interspace and stronger contrast (marked with red arrows) are attributed to the interference between top and bottom crystal surfaces, which provide the information about crystal thickness.

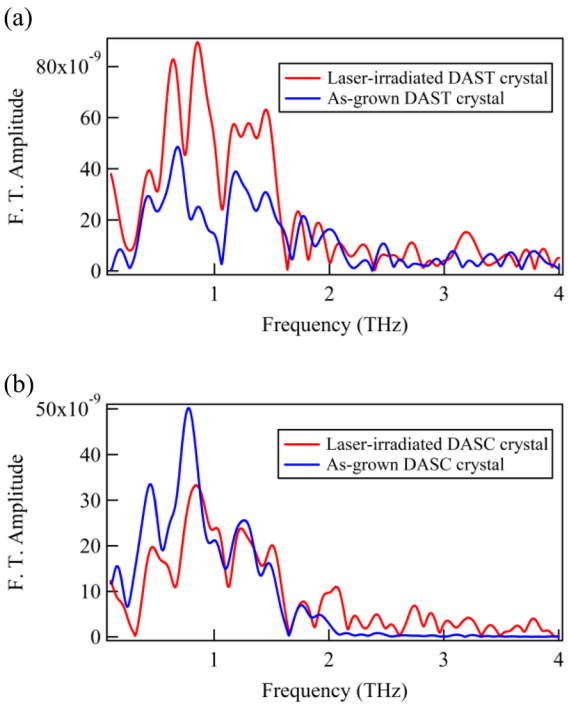

Figure 5. THz Fourier-transform spectra obtained from (a) DAST and (b) DASC crystals. Red and blue lines indicate the laser-irradiated crystals and as-grown ones, respectively. The laser parameters applied in the experiment to fabricate laser-irradiated crystal was consistent with the experimental condition in Figure 2 (shot to inward of (001) surface).

ASSOCIATED CONTENT

Supporting Information.

The following files are available free of charge.

Determination of threshold energy of laser ablation, optical setup for laser ablation and crystal observation, influence of laser ablation on crystal thickness, and crossed Nicols observation of NLO crystals (PDF).

Movie S1: Bright-field (left) and LCM-DIM (right) images of growth behavior of DAST crystals induced by the laser shot to the edge of (001) surface [Figure 1(a)] (MP4). Time in the movie is labeled as hh:mm:ss. A single fs laser pulse was shot at t = 00:00:00.

Movie S2: Bright-field (left) and LCM-RM (right) images of growth behavior of DASC crystals induced by the laser shot to the edge of (001) surface [Figure 1(b)] (MP4). Time in the movie is labeled as mm:ss. A single fs laser pulse was shot at t = 00:00.

Movie S3: Bright-field (left) and LCM-DIM (right) images of growth behavior of DAST crystals induced by the laser shot to the center of (001) surface [Figure 2(a)] (MP4). Time in the movie is labeled as hh:mm:ss. A single fs laser pulse was shot at t = 00:00:00.

Movie S4: Bright-field (left) and LCM-DIM (right) images of growth behavior of DASC crystals induced by the laser shot to the center of (001) surface [Figure 2(b)] (MP4). Time in the movie is labeled as hh:mm:ss. A single fs laser pulse was shot at t = 00:00:00.

Movie S5: Generation of spiral growth on a DAST crystal surface by laser ablation (Figure 4) (MP4).

AUTHOR INFORMATION

Notes

H. T and M. Y contributed equally to this work.

The authors declare no competing financial interests.

ACKNOWLEDGMENT

This work was partly supported by grants from the Japan Society for the Promotion of Science (JSPS) KAKENHI (Nos: 19H02613, 19KK0128, 20K21117 to H.Y.Y and JP16H06507 to T.S.), and the Ministry of Science and Technology in Taiwan (MOST 109-2113-M-009-008- and 109-2927-I-009-513 to T.S.). This work was also supported by the joint research project of Institute of Laser Engineering, Osaka University (2020B2-015) and by Center for Emergent Functional Matter Science of National Yang Ming Chiao Tung University from The Featured Areas Research Center Program within the framework of the Higher Education Sprout Project by the Ministry of Education (MOE) in Taiwan.

REFERENCES

1. Kwon, O. P.; Kwon, S. J.; Jazbinsek, M.; Brunner, F. D. J.; Seo, J. I.; Hunziker, C.; Schneider, A.; Yun, H.; Lee, Y. S.; Gunter, P. Organic Phenolic Configurationally Locked Polyene Single Crystals for Electro-optic and Terahertz Wave Applications. *Adv. Funct. Mater.* **2008,** *18*, 3242-3250.

2. Pan, F.; Wong, M. S.; Bosshard, C.; Gunter, P. Crystal growth and characterization of the organic salt 4-N,N-dimethylamino-4'-N'-methyl-stilbazolium tosylate (DAST). *Adv. Mater.* **1996,** *8*, 592-595.

3. Sohma, S.; Takahashi, H.; Taniuchi, T.; Ito, H. Organic nonlinear optical crystal DAST growth and its device applications. *Chem. Phys.* **1999,** *245*, 359-364.

4. Takahashi, Y.; Adachi, H.; Taniuchi, T.; Takagi, M.; Hosokawa, Y.; Onzuka, S.; Brahadeeswaran, S.; Yoshimura, M.; Mori, Y.; Masuhara, H.; Sasaki, T.; Nakanishi, H. Organic nonlinear optical DAST crystals for electro-optic measurement and terahertz wave generation. *J. Photochem. Photobiol. A: Chem.* **2006,** *183*, 247-252.

5. Matsukawa, T.; Yoshimura, M.; Takahashi, Y.; Takemoto, Y.; Takeya, K.; Kawayama, I.; Okada, S.; Tonouchi, M.; Kitaoka, Y.; Mori, Y.; Sasaki, T. Bulk Crystal Growth of Stilbazolium Derivatives for Terahertz Waves Generation. *Jpn. J. Appl. Phys.* **2010,** *49*, 075502.

6. Brahadeeswaran, S.; Takahashi, Y.; Yoshimura, M.; Tani, M.; Okada, S.; Nashima, S.; Mori, Y.; Hangyo, M.; Ito, H.; Sasaki, T. Growth of Ultrathin and Highly Efficient Organic Nonlinear Optical Crystal 4 '-Dimethylamino-N-methyl-4-Stilbazolium p-Chlorobenzenesulfonate for Enhanced Terahertz Efficiency at Higher Frequencies. *Cryst. Growth Des.* **2013,** *13*, 415-421.

7. Serita, K.; Mizuno, S.; Murakami, H.; Kawayama, I.; Takahashi, Y.; Yoshimura, M.; Mori, Y.; Darmo, J.; Tonouchi, M. Scanning laser terahertz near-field imaging system. *Opt. Express* **2012,** *20*, 12959-12965.

8. Mineno, Y.; Matsukawa, T.; Ikeda, S.; Taniuchi, T.; Nakanishi, H.; Okada, S.; Adachi, H.; Yoshimura, M.; Mori, Y.; Sasaki, T. Single crystal preparation of DAST for terahertz-wave generation. *Mol. Cryst. Liq. Cryst.* **2007,** *463*, 337-343.

9. Ruiz, B.; Jazbinsek, M.; Gunter, P. Crystal Growth of DAST. *Cryst. Growth Des.* **2008,** *8*, 4173-4184.

10. Tominaga, Y.; Maruyama, M.; Yoshimura, M.; Koizumi, H.; Tachibana, M.; Sugiyama, S.; Adachi, H.; Tsukamoto, K.; Matsumura, H.; Takano, K.; Murakami, S.; Inoue, T.; Yoshikawa, H. Y.; Mori, Y. Promotion of protein crystal growth by actively switching crystal growth mode via femtosecond laser ablation. *Nat Photonics* **2016,** *10*, 723-+.

11. Suzuki, D.; Nakabayashi, S.; Yoshikawa, H. Y. Control of Organic Crystal Shape by Femtosecond Laser Ablation. *Cryst. Growth Des.* **2018,** *18*, 4829-4833.

12. Wu, C. S.; Ikeyama, J.; Nakabayashi, S.; Sugiyama, T.; Yoshikawa, H. Y. Growth Promotion of Targeted Crystal Face by Nanoprocessing via Laser Ablation. *J. Phys. Chem. C* **2019,** *123*, 24919-24926.

13. Tsukamoto, K. In-situ observation of crystal growth and the mechanism. *Prog. Cryst. Growth Charact. Mater.* **2016,** *62*, 111-125.

14. Glavcheva, Z.; Umezawa, H.; Mineno, Y.; Odani, T.; Okada, S.; Ikeda, S.; Taniuchi, T.; Nakanishi, H. Synthesis and properties of i-methyl-4-{2-[4-(dimethylamino)phenyl]ethenyl}pyridinium p-toluenesulfonate derivatives with isomorphous crystal structure. *Jpn. J. Appl. Phys.* **2005,** *44*, 5231-5235.

15. Yoshikawa, H. Y.; Hosokawa, Y.; Masuhara, H. Spatial control of urea crystal growth by focused femtosecond laser irradiation. *Cryst. Growth Des.* **2006,** *6*, 302-305.

16. Sazaki, G.; Matsui, T.; Tsukamoto, K.; Usami, N.; Ujihara, T.; Fujiwara, K.; Nakajima, K. In situ observation of elementary growth steps on the surface of protein crystals by laser confocal microscopy. *J. Cryst. Growth* **2004,** *262*, 536-542.

17. Sazaki, G.; Zepeda, S.; Nakatsubo, S.; Yokoyama, E.; Furukawa, Y. Elementary steps at the surface of ice crystals visualized by advanced optical microscopy. *Proc. Natl. Acad. Sci. U. S. A.* **2010,** *107*, 19702-19707.

18. Qiu, H. S.; Kato, K.; Hirota, K.; Sarukura, N.; Yoshimura, M.; Nakajima, M. Layer thickness dependence of the terahertz emission based on spin current in ferromagnetic heterostructures. *Opt. Express* **2018,** *26*, 15247-15254.

19. Nakajima, M.; Kurihara, T.; Tadokoro, Y.; Kang, B.; Takano, K.; Yamaguchi, K.; Watanabe, H.; Oto, K.; Suemoto, T.; Hangyo, M. Application of Terahertz Field Enhancement Effect in Metal Microstructures. *J Infrared Millim Te* **2016,** *37*, 1199-1212.

20. Nakajima, M.; Namai, A.; Ohkoshi, S.; Suemoto, T. Ultrafast time domain demonstration of bulk magnetization precession at zero magnetic field ferromagnetic resonance induced by terahertz magnetic field. *Opt. Express* **2010,** *18*, 18260-18268.

21. Hong, H. K.; Park, J. W.; Lee, K. S.; Yoon, C. S. Growth of highly nonlinear optical organic crystal, 3-methyl-4-methoxy-4 '-nitrostilbene (MMONS). *J. Cryst. Growth* **2005,** *277*, 509-517.

22. Markov, I. *CRYATAL GROWTH FOR BEGINNERS: Fundamentals of Nucleation, Crystal Growth and Epitaxy*. World Scientific Publishing: Singapore, 2003.

23. Van Driessche, A. E. S.; Sazaki, G.; Otalora, F.; Gonzalez-Rico, F. M.; Dold, P.; Tsukamoto, K.; Nakajima, K. Direct and noninvasive observation of two-dimensional nucleation behavior of protein crystals by advanced optical microscopy. *Cryst. Growth Des.* **2007,** *7*, 1980-1987.

24. Matsukawa, T.; Mineno, Y.; Odani, T.; Okada, S.; Taniuchi, T.; Nakanishi, H. Synthesis and terahertz-wave generation of mixed crystals composed of 1-methyl-4-{2-[4-(dimethylamino)phenyl]ethenyl}pyridinium p-toluenesulfonate and p-chlorobenzenesulfonate. *J. Cryst. Growth* **2007,** *299*, 344-348.

25. Taniuchi, T.; Ikeda, S.; Mineno, Y.; Okada, S.; Nakanishi, H. Terahertz properties of a new organic crystal, 4'-dimethylamino-N-methyl-4-stilbazolium p-chlorobenzenesulfonate. *Jpn. J. Appl. Phys.* **2005,** *44*, L932-L934.

TOC image

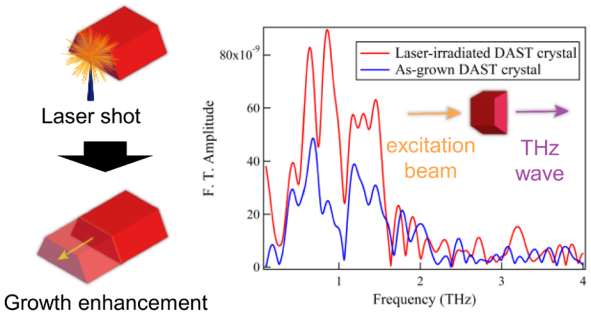

TOC Graphic